

## A Novel 1D-AF Hybrid Organic–Inorganic Chromium(II) Methyl Phosphonate Dihydrate: Synthesis, X-Ray Crystal and Molecular Structure, and Magnetic Properties

Elvira M. Bauer,<sup>\*†</sup> Carlo Bellitto,<sup>†</sup> Patrizia Imperatori,<sup>†</sup> Guido Righini,<sup>†</sup> Marcello Colapietro,<sup>‡</sup> Gustavo Portalone,<sup>\*\*†</sup> and Carlos J. Gómez-García<sup>\*§</sup>

<sup>†</sup>Consiglio Nazionale delle Ricerche, Istituto di Struttura della Materia, Via Salaria km 29.300, P.O. Box 10, 00015 Monterotondo (RM), Italy, <sup>‡</sup>Department of Chemistry, University of Rome “Sapienza”, P.le A. Moro 5, 00185 Roma, Italy, and <sup>§</sup>Instituto de Ciencia Molecular (ICMol), Parque Científico, Universidad de Valencia, 46980 Paterna, Valencia, Spain

Received May 12, 2010

Light-blue crystals of chromium(II) methyl phosphonate dihydrate,  $[\text{Cr}(\text{CH}_3\text{PO}_3)(\text{H}_2\text{O})] \cdot \text{H}_2\text{O}$ , were obtained in water by mixing filtered solutions of methylphosphonic acid and chromium(II) chloride in the presence of urea in an inert atmosphere. The compound was characterized by elemental analysis, TGA-DSC, X-ray crystallography, magnetic measurements, and UV–visible and FT-IR spectroscopies. The crystal and molecular structures (orthorhombic *Pnma* (no. 62):  $a=4.4714(5)$  Å,  $b=6.8762(7)$  Å,  $c=19.180(2)$  Å,  $Z=4$ ) have been solved using single-crystal X-ray diffraction. The chromium(II) ion is six-coordinated by oxygens (4 + 2) to form an elongated octahedron, with the four equatorial oxygen atoms belonging to  $[-\text{PO}_3]^{2-}$  phosphonate groups. This stereochemistry of the Cr(II) ion (high-spin  $d^4$  electronic configuration) is ascribed to the Jahn–Teller effect. The  $[\text{CrO}_6]$  chromophore, the  $[\text{CH}_3\text{PO}_3]^{2-}$  anions, and the water molecules build a novel one-dimensional (1D) metal(II) oxide chain, anchored to each other within the *ab* plane by two oxygens of the phosphonate ligand. Within the chain, each  $\text{Cr}^{2+}$  ion is connected through double oxygen bridges to its two neighbors, forming edge-sharing octahedra running along the *b* axis. The chains are further connected with the adjacent chains by phosphonate  $[-\text{PO}_3]^{2-}$  groups of the ligand, forming an inorganic layer that alternates along the *c* axis of the unit cell with bilayers, consisting of methyl groups and water of crystallization. The thermal variation of the magnetic susceptibility follows the Curie–Weiss law, with a large negative Weiss constant,  $\theta = -60$  K, indicating the presence of antiferromagnetic AF exchange interactions between neighboring Cr(II) ions. The magnetic behavior and the magnetic dimensionality have been analyzed in terms of Fisher’s classical limiting form of the Heisenberg chain theory, and a value of  $J = -9.3 \text{ cm}^{-1}$  was found. The negative value of the *intra*-chain exchange constant coupling  $J$  confirms the presence of an AF coupling. No sign of long-range magnetic ordering down to 2 K (the lowest measured temperature) is observed, in agreement with the predominant one-dimensional character of the exchange interactions.

### Introduction

The study of magnetic phenomena in hybrid organic–inorganic compounds is at the forefront of solid state science research, because of the interesting physical and chemical properties exhibited.<sup>1</sup> The design and the synthesis of this class of compounds in fact have provided examples of novel multifunctional materials, such as multiferroics,<sup>2</sup> ferromagnetic

conductors,<sup>3</sup> chiral magnets,<sup>4</sup> porous magnetic materials,<sup>5</sup> chiral molecular conductors,<sup>6</sup> paramagnetic superconductors,<sup>7</sup> etc., that are difficult to find in classical inorganic materials.

\*To whom correspondence should be addressed: E-mail: elvira.bauer@ism.cnr.it (E.M.B.), g.portalone@caspur.it (G.P.); carlos.gomez@uv.es (C.J.G.).

(1) See, for example, the series: *Magnetism: Molecules to Materials*; Miller, J. S., Drillon, M., Eds.; Wiley-VCH: Weinheim, Germany, 2001–2005; Vols. 1–5.

(2) Jain, P.; Ramachandran, V.; Clark, R. J.; Zhou, H. D.; Toby, B. H.; Dalal, N. S.; Kroto, H. W.; Cheetham, A. K. *J. Am. Chem. Soc.* **2009**, *131*, 13625–13627.

(3) Coronado, E.; Galán-Mascarós, J. R.; Gómez-García, C. J.; Laukhin, V. *Nature* **2000**, *408*, 447–449.

(4) (a) Kumagai, H.; Inoue, K. *Angew. Chem., Int. Ed.* **1999**, *38*, 1601–1603. (b) Clemente-Leon, M.; Coronado, E.; Dias, J. C.; Soriano-Portillo, A.; Willett, R. D. *Inorg. Chem.* **2008**, *47*, 6458–6463. (c) Coronado, E.; Gómez-García, C. J.; Nuez, A.; Romero, F. M.; Rusanov, E.; Stoeckli-Evans, H. *Inorg. Chem.* **2002**, *41*, 4615–4617. (d) Coronado, E.; Gómez-García, C. J.; Nuez, A.; Romero, F. M.; Waerenborgh, J. C. *Chem. Mater.* **2006**, *18*, 2670–2681.

(5) Zhang, Y.; Liu, T.; Sato, O. *J. Am. Chem. Soc.* **2010**, *132*, 912–913.

(6) Coronado, E.; Galán-Mascarós, J. R.; Gómez-García, C. J.; Murcia-Martínez, A.; Canadell, E. *Inorg. Chem.* **2004**, *43*, 8072–8077.

(7) (a) Kurmoo, M.; Graham, A. W.; Day, P.; Coles, S. J.; Hursthouse, M. B.; Caulfield, J. L.; Singleton, J.; Pratt, F. L.; Hayes, W.; Ducasse, L.; Guionneau, P. *J. Am. Chem. Soc.* **1995**, *117*, 12209–12217. (b) Kobayashi, H.; Tomita, H.; Naito, T.; Kobayashi, A.; Sakai, F.; Watanabe, T.; Cassoux, P. *J. Am. Chem. Soc.* **1996**, *118*, 368–377. (c) Coronado, E.; Curreli, S.; Giménez-Saiz, C.; Gómez-García, C. J. *J. Mater. Chem.* **2005**, *15*, 1429–1436.

One of these promising series of organic–inorganic hybrids is the paramagnetic metal(II) organo-phosphonates  $M^{II}[(RPO_3)(H_2O)]_n$ ,<sup>8</sup> where  $M(II) = Mn, Fe, Co, \text{ or } Ni$  and  $R$  is an organic group. The latter are attractive because the organic group,  $R$ , may include an additional tailored chemical or physical property. The structures of these metal phosphonates  $M^{II}[(RPO_3)(H_2O)]_n$  present alternating organic–inorganic layers where the organic group,  $R$ , of the phosphonate lies in the interlayer space forming a bilayer (thanks to van der Waals contacts) that is interspersed between the inorganic ones. Within the inorganic layer, the metal(II) ion is six coordinated by oxygen atoms in a distorted octahedral symmetry, four of them bridging neighboring metal ions. The magnetic behavior at low temperatures<sup>8</sup> is related to the 2D character of the inorganic sublattice, and interestingly, two new Ni(II) organo-phosphonates were found to be ferromagnets at low temperatures.<sup>9</sup> A few years ago, we were able to synthesize some Cr(II) organophosphonates with long-range magnetic ordering at low temperatures.<sup>10</sup> Only one of them, an organic–inorganic hybrid of formula  $Cr[(H_3N(CH_2)_2PO_3)(Cl)(H_2O)]$ , was isolated as a crystalline phase and could be structurally and physically characterized.<sup>11,12</sup> The compound was found to have a polar structure and to be a canted antiferromagnet below  $T_N = 5.5$  K. Among the large number of paramagnetic metal ions, the Cr(II) ion represents an interesting building block for the self-assembling of multifunctional magnetic hybrids, due to its high-spin  $d^4$  electron configuration. Unfortunately, its air-sensitivity has prevented the synthesis and crystal growth of new compounds. Thus, up to now, only a scarce number of Cr(II) compounds containing oxygen atoms coordinated to the metal ion have been isolated and structurally characterized.<sup>13</sup> For this reason, we have prepared several Cr(II) alkylphosphonates, and only recently we have succeeded in the single-crystal growth of one form of the first member of the series, i.e.  $[Cr(CH_3PO_3)(H_2O)] \cdot H_2O$  (**1**).

Here, we report the X-ray single-crystal structure and the magnetic properties of this chromium(II) methylphosphonate dihydrate.

## Experimental Section

**Materials and Methods.** Commercially available chemical reagents were used without further purification; i.e., methylphosphonic acid,  $CrCl_2$ , was used as supplied from Aldrich Chemical Co., and HPLC water was used as solvent. All reactions and the handling involving Cr(II) samples were carried out under an inert atmosphere by using Schlenck techniques. Water was purged with  $N_2$  gas prior to use. Elemental analyses were performed by

Malissa & Reuter Mikroanalytische Laboratorien, Elbach, Germany. Thermogravimetric (TGA) data were collected in flowing dry nitrogen at a rate of  $5^\circ C/min$  on a ThermoAnalysis Q60 thermoanalyzer. FT-IR absorption spectra were recorded on a Shimadzu Prestige 21 spectrophotometer using KBr pellets. UV–vis–NIR absorption spectra were recorded on a Perkin-Elmer 950 spectrophotometer equipped with a diffuse reflectance sphere.

The single-crystal structure of  $[Cr(CH_3PO_3)(H_2O)] \cdot H_2O$  (**1**) was determined from a selected light-blue plate-like crystal of approximately  $0.20 \times 0.1 \times 0.08$  mm<sup>3</sup> in sealed Lindeman tubes. The X-ray intensity data were collected at room temperature on a four-circle diffractometer equipped with an Xcalibur S CCD area detector, graphite monochromator, and a Mo  $K\alpha$  enhanced fine-focus sealed tube ( $\lambda = 0.71070$  Å). They were corrected for absorption effects by using CrysAlis RED.<sup>14</sup> The structure was solved by using the SIR97 package<sup>14</sup> and refined with the SHELXL-97<sup>15</sup> software.

The DC magnetic susceptibility measurements were carried out in the temperature range 2–300 K with an applied magnetic field of 0.1 T on a polycrystalline sample of compound **1** ( $m = 13.18$  mg), with a Quantum Design MPMS-XL-5 SQUID magnetometer. The isothermal magnetization was measured on the same sample at 2 K with magnetic fields up to 9 T with a Quantum Design PPMS-9 equipment. The AC magnetic measurements were performed on a sample composed by several single crystals ( $m = 0.34$  mg) with an alternating field of 0.395 mT in the frequency range 1–1000 Hz in the MPMS-XL-5 SQUID susceptometer. The susceptibility data were corrected for the sample holders previously measured using the same conditions and for the diamagnetic contributions of the salt as deduced by using Pascal's constant tables ( $\chi_{dia} = -94.4 \times 10^{-6}$  emu mol<sup>-1</sup>).<sup>16</sup> The temperature-independent susceptibility,  $\chi_{up}$ , was corrected from the usual expression by assuming that, with  $O_h$  symmetry for Cr(II) ( $S = 2$ ), the <sup>3</sup>D splits to yield the <sup>3</sup>E ground state:  $\chi_{up} = 4N\mu_B^2/10Dq$ , where  $10Dq = 11\,700$  cm<sup>-1</sup> from the electronic spectrum.

**Synthesis of Chromium(II) Methylphosphonate,  $[Cr(CH_3PO_3)(H_2O)] \cdot H_2O$  (**1**).** Compound **1** was prepared by mixing filtered aqueous solutions of methylphosphonic acid and  $CrCl_2$  in the presence of urea in a pyrex ampoule under an inert atmosphere. The latter was sealed and kept at  $80^\circ C$  in an oven for two days. The light-blue microcrystalline precipitate that formed was filtered off under nitrogen, washed several times with degassed water, and then dried under vacuum. The Cr(II) methyl derivative slowly decomposes in the air. The composition of the material was checked by elemental analyses and by TGA measurements. Elemental analysis calcd. (%) for  $CH_7CrPO_5$ : C, 6.60; H, 3.87; Cr, 28.56; P, 17.01. Found (%): C, 7.03; H, 3.34; Cr, 29.60; P, 13.95.

Please Note: The low phosphorus content detected by elemental analysis can be explained taking into account the proposed molecular formula and detected values for Cr and the ligand. The C/P atomic ratio in the ligand is 1:1, and as a consequence the ratio  $Cr/C/P = 1$ , which means that the ratio  $Cr/ligand = 1$ . The detected value of the %C/atomic weight ratio is 0.586, and the detected value of the %Cr/atomic weight ratio is 0.569, the latter being quite close to the above-reported value. This suggests that during the determination process of %P some phosphorus has been lost. However, structural studies confirmed the stoichiometry of the analyzed compound.

(8) (a) Carling, S. G.; Day, P.; Visser, D. J. *Solid State Chem.* **1993**, *106*, 111–119. (b) Clearfield, A. *Prog. Inorg. Chem.* **1998**, *47*, 371–510. (c) Bellitto, C. In *Magnetism: Molecules to Materials*; Miller, J. S., Drillon, M., Eds.; Wiley-VCH: Weinheim, Germany, 2001; Vol. 2, p 425–456. (d) Bellitto, C.; Bauer, E. M.; Righini, G. *Inorg. Chim. Acta* **2008**, *361*, 3785–3799.

(9) (a) Bauer, E. M.; Bellitto, C.; Gómez García, C. J.; Righini, G. *J. Solid State Chem.* **2008**, *181*, 1213–1219. (b) Bauer, E. M.; Bellitto, C.; Colapietro, M.; Drillon, M.; Portalone, G.; Rabu, P.; Righini, G. *Inorg. Chem.* **2008**, *47*, 10945–10952.

(10) (a) Bellitto, C.; Federici, F.; Ibrahim, S. A. *J. Chem. Soc. Chem. Commun.* **1996**, 759–760. (b) Bellitto, C.; Federici, F.; Ibrahim, S. A. *Chem. Mater.* **1998**, *10*, 1076–1082.

(11) Bauer, E. M.; Bellitto, C.; Colapietro, M.; Portalone, G.; Righini, G. *Inorg. Chem.* **2003**, *42*, 6345–6351.

(12) Nénert, G.; Adem, U.; Bauer, E. M.; Bellitto, C.; Righini, G.; Palstra, T. T. *Phys. Rev.* **2008**, *B78*, 54443(5).

(13) (a) Stock, N.; Ferey, G.; Cheetham, A. K. *Solid State Sci.* **2000**, 307–312. (b) Schmidt, A.; Glaum, R. *Inorg. Chem.* **1997**, *36*, 4883–4887.

(14) (a) *CrysAlis CCD*; *CrysAlis RED*, version 1.171.32.3; Oxford Diffraction Ltd.: Abingdon, Oxfordshire, England, 2006. (b) Altomare, A.; Burla, M. C.; Camalli, M.; Cascarano, G.; Giacovazzo, C.; Guagliardi, A.; Moliterni, A. G. G.; Polidori, G.; Spagna, R. *J. Appl. Crystallogr.* **1999**, *32*, 115. (c) Sheldrick, G. M. *Acta Crystallogr.* **2008**, *A64*, 112–122.

(15) Sheldrick, G. M. *SHELXL-97*; University of Göttingen; Göttingen, Germany, 1997.

(16) See, for example: Carlin, R. L. *Magnetochemistry*; Springer-Verlag: Berlin, 1986.

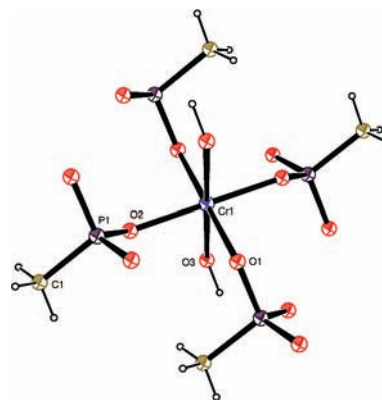
**Table 1.** Crystal Data and Data Collection for Compound  $[\text{Cr}(\text{CH}_3\text{PO}_3)(\text{H}_2\text{O})] \cdot \text{H}_2\text{O}$  (1)

chemical formula	$\text{CH}_7\text{CrO}_5\text{P}$
$M_r$	182.03
cell setting, space group	orthorhombic, $Pnma$
temp (K)	298(2)
$a, b, c$ (Å)	4.4714(5), 6.8762(7), 19.180(2)
$V$ (Å <sup>3</sup> )	589.73(11)
$D_x$ (Mg m <sup>-3</sup> )	2.028
radiation type	Mo K $\alpha$ , 0.71070 Å
$M$ (cm <sup>-1</sup> )	21.5
cryst form, color	blue
cryst size (mm)	0.20 × 0.1 × 0.08
Data Collection	
diffractometer	Oxford Diffraction Xcalibur S CCD
data collection method	$\Omega$ and $\Phi$
adsorption correction	multiscan (based on symmetry-related measurements)
$T_{\text{min}}$	0.6732
$T_{\text{max}}$	0.8469
no. of measured, independent, and observed reflection [ $F^2 > 2\sigma(F^2)$ ]	1817, 662, 532
$R_{\text{int}}$	0.0224
$\Theta_{\text{max}}$ (deg)	26.5
Refinement	
Refinement on $R[F^2 > 2\sigma(F^2)]$ , $wR(F^2)$ , $S$	$F^2$ 0.0402, 0.1078, 1.157
no. of params	57
H-atom treatment	refined
$(\Delta/\sigma)_{\text{max}}$	0.000
$\Delta\rho_{\text{max}}, \Delta\rho_{\text{min}}$ (Å <sup>-3</sup> )	0.7(1), -0.7(1)

## Results and Discussion

Single crystals of Cr(II) methylphosphonate dihydrate have been isolated by the reaction of methylphosphonic acid and  $\text{CrCl}_2$  in water under an inert atmosphere. The preparation was carried out in the presence of urea at temperatures slightly above 80 °C in a sealed ampule. Under these conditions, the urea slowly hydrolyzes with the release of ammonia and, therefore, increasing the pH of the solution. The isolated compound is light-blue and crystallizes as plate-like crystals. The thermogravimetric analysis of  $[\text{Cr}(\text{CH}_3\text{PO}_3)(\text{H}_2\text{O})] \cdot \text{H}_2\text{O}$  features three mass losses (see the Supporting Information, Figure S1). The first step, at 60 °C, presents a mass loss of 1.5%. The second one takes place in the temperature range 100–200 °C and represents a mass loss of 8.5%. The apparent discrepancy between the TGA data and the crystallization water content (see below) can be explained by the low value of the temperature at which the compound starts to lose water (below 40 °C). The second step is related to the loss of coordinated water. The observed total loss of 10.0% corresponds to the removal of one water molecule per formula unit. The final mass loss observed between 450 and 622 °C results from the decomposition of the organic ligand, and it is an indication of the high thermal stability of the compound.

**Crystal Structure of  $[\text{Cr}(\text{CH}_3\text{PO}_3)(\text{H}_2\text{O})] \cdot \text{H}_2\text{O}$  (1).** The title compound crystallizes in the orthorhombic space group  $Pnma$  and shows a hybrid inorganic–organic structure, where the inorganic layers alternate with the organic bilayers along the  $c$  axis. Details of the crystal data collection, structure solution, and refinement are reported in Table 1. The asymmetric unit consists of one Cr atom, located on an inversion center and four methylphosphonate ligands (see Figure 1). The geometry around the Cr(II) ion is an elonga-

**Figure 1.** Monomeric structure of the title compound with atomic labeling scheme (thermal ellipsoids to 50% probability).**Table 2.** Selected Bond Length (Å) and Angles (deg) for Compound  $[\text{Cr}(\text{CH}_3\text{PO}_3)(\text{H}_2\text{O})] \cdot \text{H}_2\text{O}$  (1)

Cr–O1	2.084(2)	P1–O1	1.553(4)
Cr–O2	2.031(2)	P1–O2	1.521(2)
Cr–O3	2.606(2)		
P1–C1	1.800(6)		
O1–Cr–O2	89.3(1)	O1–Cr–O1	180.0(2)
O1–Cr–O2	90.7(1)	O2–Cr–O2	180.0(1)
Cr–O3–Cr	82.5(1)		

ted octahedron with four in-plane, equatorial, short Cr–O bonds (Cr–O1 = 2.084(2) Å, Cr–O2 = 2.031(2) Å, from four adjacent phosphonate groups) and two long, axial Cr–O bonds (Cr–O3 = 2.607(2) Å, from the water molecules). Selected bond length and angles are reported in Table 2. These bond distances are similar to those observed in  $\text{Na}_2\text{CrP}_2\text{O}_7$ ,<sup>13</sup> although in the latter the coordination is five. The difference between the equatorial and the axial Cr–O distances can be attributed to the Jahn–Teller effect, operating in Cr(II) high spin ( $S = 2$ ) systems.<sup>16</sup> The *cis* O–Cr–O bond angles also deviate from 90° (they are in the range 82–97°), confirming the presence of a distortion in the Cr(II) octahedron.

These  $[\text{CrO}_6]$  octahedra form chains along the  $b$  axis containing inclined edge-sharing octahedra, with a small Cr–O3–Cr angle of 82.5(1)° and a large Cr–O1–Cr angle of 111.2(2)°, as a result of the Jahn–Teller elongation of the Cr–O3 bond. The chains are further connected with the adjacent chains by phosphonate groups  $[-\text{PO}_3]^{2-}$  of the ligand, thus forming an inorganic layer in the  $ab$  plane (see Figure 2a). The O1 atom of the phosphonate group connects two adjacent Cr(II) ions, while the other two oxygen atoms of the  $[-\text{PO}_3]^{2-}$  group (O2 and O2<sup>#</sup>) are bonded to the Cr(II) ions located on adjacent chains; thus, they connect the chains through  $-\text{O}-\text{P}-\text{O}-$  bridges. The intrachain Cr–Cr distance (3.438(2) Å) is significantly shorter than the interchain one (4.472(2) Å). The  $-\text{CH}_3$  group, located opposite the  $[-\text{PO}_3]^{2-}$  group, is orientated almost perpendicular to the inorganic layers and situated between them, forming an organic bilayer. The crystallization water molecules are located in the cavities left by the adjacent  $-\text{CH}_3$  groups in the interplanar space (Figure 2b) and are held together by hydrogen bonds.

In summary, the structure of compound 1 can be described as being formed by chains of inclined edge-sharing elongated octahedra with almost orthogonal equatorial planes. The chains are interconnected through  $-\text{O}-\text{P}-\text{O}-$  bridges to

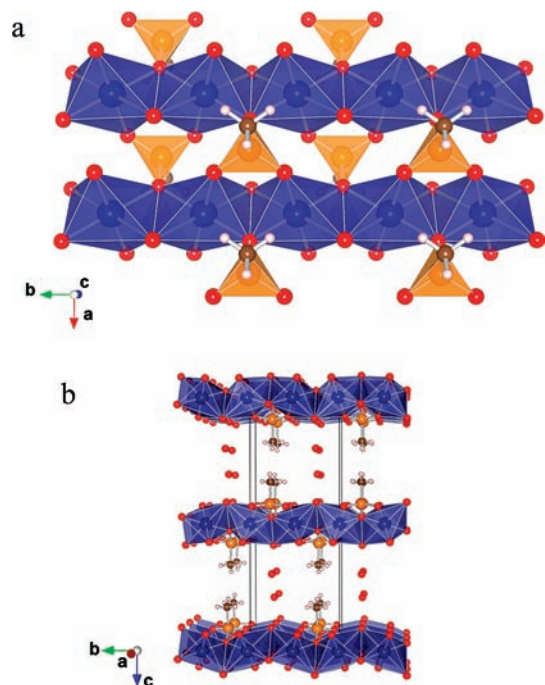


**Figure 2.** (a) Polyhedral view of the structure of the inorganic layer in the title compound. (b) Unit-cell packing of  $[\text{Cr}(\text{CH}_3\text{PO}_3)(\text{H}_2\text{O})]\cdot\text{H}_2\text{O}$  viewed along the  $a$  axis. Color code: Cr = blue, P = orange, O = red, C = brown, H = light pink.

form inorganic layers, which are interspersed along the  $c$  axis with the organic bilayers.

**Optical Properties. IR Spectra.** The FT-IR absorption spectrum of  $[\text{Cr}(\text{CH}_3\text{PO}_3)(\text{H}_2\text{O})]\cdot\text{H}_2\text{O}$  features, in the  $3700\text{--}3200\text{ cm}^{-1}$  region, a broad and intense band with the maximum centered at about  $3440\text{ cm}^{-1}$  and two superposed sharp and intense peaks at  $3590\text{ cm}^{-1}$  and  $3497\text{ cm}^{-1}$ , which could be assigned to the O–H stretching modes of the water molecules (see the Supporting Information, Figure S2). These assignments are reminiscent of what have been observed in the beryl mineral.<sup>17</sup> In the latter study, polarized IR spectra of hydrated synthetic beryl have been compared to the natural one in order to identify the type of water molecules present in the lattice, i.e., crystallization water molecules or coordinated water molecules. Here, according to the structure of compound **1**, both types of water molecules are present in the lattice. The sharpest peak at  $3497\text{ cm}^{-1}$  can be assigned to the stretching vibration of coordinated water, while the other one at higher wave numbers ( $3590\text{ cm}^{-1}$ ) is possibly due to the water of crystallization. The  $\text{H}_2\text{O}$  bending modes associated with these two types of water molecules appear in the range between  $1630\text{ cm}^{-1}$  and  $1600\text{ cm}^{-1}$ . The C–H stretching bands of the methyl group of the ligand are located at  $2995\text{ cm}^{-1}$  and  $2925\text{ cm}^{-1}$ , respectively. Four bands due to the  $[-\text{PO}_3]^{2-}$  group vibrations are observed in the range  $1200\text{--}900\text{ cm}^{-1}$ . The complete conversion of the acid into the Cr(II) compound is demonstrated by the absence of OH stretching of the P–OH group at about  $2700\text{--}2550\text{ cm}^{-1}$  and  $2350\text{--}2100\text{ cm}^{-1}$ .

**UV–Visible Spectra.** The diffuse reflectance electronic spectrum of compound **1** has been recorded, and it is reported in the Supporting Information (Figure S3). It features a

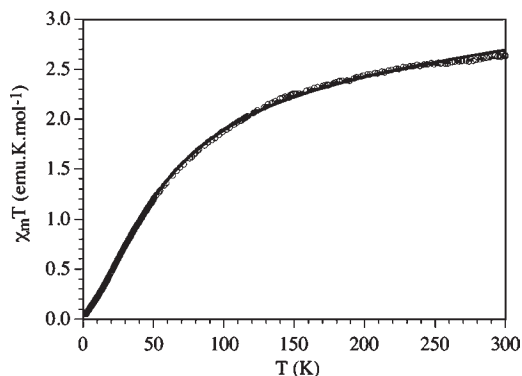


**Figure 3.** Thermal variation of the  $\chi_m T$  product for compound **1**. Solid and dashed lines are the best fit to the models (see text).

very broad band with two maxima at 825 and 620 nm; a shoulder at 735 nm; spin-forbidden bands at 520, 424, 378 and 320 nm; and finally an intense band with a maximum centered at 230 nm. This spectrum is compatible with the presence of an octahedral  $[\text{CrO}_6]$  and is very similar to those of the salts  $\text{K}_2\text{SO}_4\cdot\text{CrSO}_4\cdot 2\text{H}_2\text{O}$ <sup>18a</sup> and  $\text{CrSO}_4\cdot 5\text{H}_2\text{O}$ ,<sup>18b</sup> containing a tetragonal distorted  $[\text{Cr}(\text{H}_2\text{O})_6]^{2+}$  ion. The splitting of the  $^5\text{D}$  term of the free  $\text{Cr}^{2+}$  ion ( $3d^4$ ) in a weak octahedral field would lead to an upper  $^5\text{T}_{2g}$  level and to a lower  $^5\text{E}_g$  level, and therefore, one spin-allowed transition is expected. However, the  $^5\text{E}_g$  ground state is orbitally degenerate in  $\text{O}_h$  symmetry, and the compound is subject to the Jahn–Teller distortion, which distorts to a tetragonal elongated octahedron ( $\text{D}_{4h}$ ), and three spin allowed electronic transitions are expected in the NIR and visible region. A similar behavior has been observed in some 1D and 2D ionic magnetic chromium(II) halides of the types  $\text{CrCl}_2$ ,  $\text{CsCrCl}_3$ ,  $(\text{R}_4\text{N})\text{CrCl}_3$ , and  $(\text{RNH}_3)_2\text{CrCl}_4$ .<sup>19</sup>

**Magnetic Properties.** The magnetic susceptibility measurements of compound **1** made on a microcrystalline sample and on single crystals show identical behaviors, confirming the identity of both samples. In the following, the measurements done on the polycrystalline sample will be discussed, since the higher mass of this sample allows more accurate measurements. As can be seen in Figure 3, the thermal variation of the product of the molar magnetic susceptibility times the temperature,  $\chi_m T$ , per Cr(II) ion shows a room temperature value of ca.  $2.65\text{ cm}^3\cdot\text{K}\cdot\text{mol}^{-1}$ , which is the expected one for a high-spin Cr(II) ion ( $d^4$ ,  $S = 2$ ) configuration with a  $g$  of ca. 1.9. On lowering the temperature,  $\chi_m T$  shows a gradual decrease to reach a value close to zero at low temperatures. This behavior clearly indicates the presence of dominant antiferromagnetic interactions in compound **1** that can, in principle, be attributed to the presence of intrachain Cr–Cr interactions. The antiferromagnetic nature of the Cr–Cr interactions are confirmed by the presence of a rounded maximum in the  $\chi_m$  versus  $T$  plot at ca. 35 K (see Figure 4). Below this temperature,  $\chi_m$  shows a gradual decrease to

(18) (a) Earnshaw, A.; Larkworthy, L. F.; Patel, K. C. *J. Chem. Soc. A* **1965**, 3267–3271. (b) Earnshaw, A.; Larkworthy, L. F.; Patel, K. C.; Beech, G. *J. Chem. Soc. A* **1969**, 1334–1339. (c) Hitchman, M. A.; Lichon, M.; McDonald, R. G.; Smith, P. W.; Strange, R.; Skelton, B. W.; White, A. H. *J. Chem. Soc. Dalton* **1987**, 1817–1822.

(19) Bellitto, C.; Brunner, H.; Güdel, H. U. *Inorg. Chem.* **1987**, *26*, 2750–2754.

(17) Fukuda, J.; Shinoda, K. *Phys. Chem. Miner.* **2008**, *35*, 347–357.

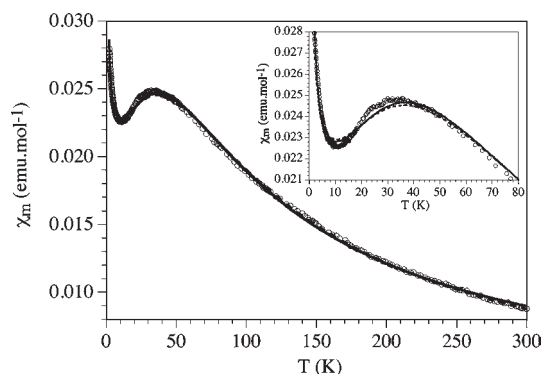


**Figure 4.** Thermal variation of  $\chi_m$  for compound **1**. Solid and dashed lines are the best fit to the models (see text). The inset shows the low-temperature region.

reach a minimum at ca. 11 K and a divergence at lower temperatures (see the inset in Figure 4). Besides the predominant intrachain antiferromagnetic interactions, this plot also shows the presence of small fractions of monomeric paramagnetic impurities, responsible of the Curie tail observed at very low temperatures.

Since the structure of compound **1** can be described as Cr(II) chains with double oxo bridges that are connected through  $-\text{O}-\text{P}-\text{O}-$  bridges, we can, in a first approach, consider that the longer  $-\text{O}-\text{P}-\text{O}-$  bridges are negligible as compared to the double oxo bridges inside the chain. Accordingly, we have analyzed the magnetic data, assuming a Heisenberg linear-chain model applied to an  $S = 2$  system (Hamiltonian  $H = -J\sum S_i S_{i+1}$ ) plus a paramagnetic  $S = 2$  impurity  $c$ , with  $J$  being the intrachain magnetic exchange:<sup>20</sup>

$$\chi_{1D} = (1 - c) \frac{Ng^2\beta^2 S(S+1)}{3kT} \frac{1+u}{1-u} + c \frac{2Ng^2\beta^2}{kT} \quad (1)$$

where,

$$u = \coth \left[ \frac{JS(S+1)}{kT} \right] - \left[ \frac{kT}{JS(S+1)} \right]$$

This model reproduces very well the  $\chi_m$  vs  $T$  and  $\chi_m T$  vs  $T$  plots of the title compound with  $g = 1.981(8)$ ,  $J = -9.2(1) \text{ cm}^{-1}$ , and  $c = 0.50(5)\%$  of the paramagnetic  $S = 2$  impurity (dashed line in Figures 3 and 4). Note that although this model reproduces very satisfactorily the magnetic data above the maximum, in the low temperature region, the agreement between the experimental and the calculated data is less satisfying. A possible explanation for this difference may be the presence of non-negligible interchain interactions, as was assumed in a first approach. Thus, we have included a term to account for the interchain interactions by using the molecular field approximation:<sup>21</sup>

$$\chi_{1D}^{\text{mfa}} = \frac{\chi_{1D}}{1 - (2zJ'/Ng^2\beta^2)\chi_{1D}} \quad (2)$$

where  $J'$  is the interchain magnetic interaction of the  $z$  neighbors, and  $\chi_{1D}$  is the magnetic susceptibility of the

isolated chain (eq 1). This model reproduces satisfactorily the magnetic properties of compound **1** with the following parameters:  $g = 1.876(9)$ ,  $J = -9.3(4) \text{ cm}^{-1}$ ,  $J' = -1.6(1) \text{ cm}^{-1}$  (we fix  $z = 2$ , since each chain is connected to two neighboring chains), and  $c = 0.58(5) \%$  of the paramagnetic  $S = 2$  impurity (solid line in Figures 3 and 4). Note that although this model reproduces very satisfactorily the magnetic properties of the title compound, the fit in the low-temperature region is only slightly improved. The low value of the  $J/J'$  ratio (ca. 6) may be at the origin of this difference, since the molecular field approximation requires a  $J/J'$  ratio of at least 10. Furthermore, a close inspection of the interchain connections shows two different possible exchange pathways. Thus, each Cr(II) ion is connected to three Cr(II) ions of the neighboring chain through  $-\text{O}-\text{P}-\text{O}-$  bridges. The connection with the central one of these three ions is made through a double  $-\text{O}-\text{P}-\text{O}-$  bridge, whereas with the other two Cr(II) ions, the connection is made via a single  $-\text{O}-\text{P}-\text{O}-$  bridge. Finally, the magnetic model used is based on the crystal structure determined at room temperature. Interestingly, in the title compound, there is an important Jahn–Teller distortion located in the main intrachain exchange pathway. Since the thermal variation is expected to strongly affect this distortion (bond distance and angle), the magnetic coupling through it is also expected to undergo an important variation when the temperature is lowered.

As expected, both models confirm the presence of intrachain antiferromagnetic interactions and of a small amount of paramagnetic impurities. In order to explain the magnitude and sign of the intrachain coupling,  $J$ , we have to consider the previous magneto-structural correlations established for double oxo-bridged metal ions. Although such correlations have not been done for Cr(II) ions (given the very reduced number of oxo-bridged Cr(II) complexes), we can use the ones established for Cu(II) complexes ( $d^9$ ) since in both ions the magnetic orbital is the  $e_g$  ( $d_{z^2}$ ). These correlations indicate that the main parameters determining the magnetic coupling are the M–O bond distance and the M–O–M bond angle.<sup>22</sup> Two very different oxo bridges (the water molecule, O3, corresponding to the Jahn–Teller elongated axis and a phosphonate oxygen atom, O1) are present in the title compound. The structural parameters of these two oxo bridges (Cr–O1 = 2.084(2) Å and Cr–O3 = 2.607(2) Å with Cr–O3–Cr and Cr–O1–Cr bond angles of 82.5(1)° and 111.18(15)°, respectively) indicate that the magnetic coupling through them should be weak and antiferromagnetic in both cases, in agreement with the experimental value found in the title compound. Unfortunately, the title compound **1** is the only magnetically characterized 1D Cr(II) complex with a double oxo bridge, and therefore, neither a comparative study nor magneto-structural correlation can be done.

Finally, in order to check the presence of any long-range ordering at low temperatures (due to a spin canting inside the chain as a consequence of the Jahn–Teller distortion and/or the inclination of the Cr(II) octahedra), AC measurements at different frequencies and isothermal

(20) (a) Fisher, M. E. *Am. J. Phys.* **1964**, *32*, 343–346. (b) Smith, T.; Friedberg, S. A. *Phys. Rev.* **1968**, *176*, 660–665.

(21) O'Connor, C. J. *Prog. Inorg. Chem.* **1982**, *29*, 203.

(22) Chiari, B.; Helms, J. H.; Piovesana, O.; Tarantelli, T.; Zanazzi, P. F. *Inorg. Chem.* **1986**, *25*, 2408–2413.

hysteresis measurements at  $T = 2$  K have been performed (see the Supporting Information, Figure S4). These measurements show no sign of long-range ordering (no AC peaks and no hysteresis cycles are observed above 2 K).<sup>23</sup>

### Conclusions

A novel crystalline form of Cr(II) methylphosphonate dihydrate has been synthesized and structurally characterized. Unlike most Cr(II) phosphonates, the crystals were of sufficient size and of quality to allow single-crystal structure determination by X-ray diffraction. The title compound is layered, but it features a different crystal structure from those of Mn(II), Fe(II), Ni(II), and Co(II) analogues. The chromium(II) ion is six-coordinated by oxygens (4 + 2) to form an elongated octahedron. This stereochemistry of the Cr(II) ion (high-spin  $d^4$  configuration) is due to the Jahn–Teller effect, which also affects the magnetic properties. The  $[\text{CrO}_6]$  chromophore, the  $[\text{CH}_3\text{PO}_3]^{2-}$  ligand and a water molecule build unprecedented one-dimensional metal oxide chains where each  $\text{Cr}^{2+}$  octahedron is connected to its two neighbors, forming edge-sharing octahedra running along the  $b$  axis. The chains are connected with the neighboring ones by phosphonate groups, thus forming inorganic layers parallel to the  $ab$  plane that alternate along the  $c$  axis with bilayers containing the methyl groups of the ligand and water

of crystallization, the latter held together by a H-bonding network. This is, to our knowledge, the first example of a one-dimensional chromium(II) oxide polymer bridged by phosphonate anions and by a water molecule.

The magnetic properties of this new compound show one-dimensional AF magnetic behavior with weak antiferromagnetic intrachain exchange interactions ( $J = -9.3(4) \text{ cm}^{-1}$ ) that can be attributed to a Cr(II)–Cr(II) interaction through the double oxo bridge via a superexchange mechanism. At low temperatures, no long-range magnetic order is observed. This behavior can be rationalized on the basis of the 1D character of the crystal structure.

**Acknowledgment.** We acknowledge support from Consiglio Nazionale delle Ricerche (Italy), the European Union (MAGMANet network of excellence and COST Action D35-WG11), the Spanish Ministerio de Educación y Ciencia (Projects MAT2007-61584 and CSD 2007-00010 Consolider-Ingenio in Molecular Nanoscience) and the Generalitat Valenciana (Project PROMETEO/2009/095). Dr. P. Plescia is acknowledged for TGA and DSC measurements.

**Supporting Information Available:** TGA/DSC measurements (Figure S1), FT-IR spectra (Figure S2), UV–vis spectra (Figure S3), AC magnetic measurements,  $\chi'$  and  $\chi''$  vs  $T$  plots in the low temperature region 2–40 K (Figure S4), and a CIF file. This material is available free of charge via the Internet at <http://pubs.acs.org>.

(23) Rojas, D. P.; Rodríguez Fernández, J.; Espeso, J. I.; Gómez Sal, J. C. *Physica B* **2009**, 2938–2941.